ISSN: 1687-1006 p
ISSN: 2682-3640 e

The Egyptian International Journal of Engineering Sciences and Technology

https://eijest.journals.ekb.eg/

Vol. 41 (2023) 56–63

DOI: 10.21608/eijest.2022.127014.1143

On the Modelling of the Dimensional Characteristics for Holes after Thermal Friction Drilling

Harbi A. E. SH. Alajmi[a], Sameh S. Mohammed[a], Tamer S. Mahmoud[a], Mohammed Abdelhameed[b*]

[a] *Mechanical Engineering Department, Faculty of Engineering at Shoubra, Benha University, Cairo 13518, Egypt.*
[b] *Mechanical Design and Production Department, Faculty of Engineering, Zagazig University, Zagazig 44519, Egypt.*

ARTICLE INFO

Article history:

Received 18 March 2022
Received in revised form
26 April 2022
Accepted 25 May 2022
Available online 25 May 2022

Keywords:

Thermal friction drilling
AA6082 aluminium alloy
Bushing thickness
Hole diameter
Artificial neural network

ABSTRACT

Thermal Friction drilling (TFD) process is a non-traditional, hole forming process that produces bushing without the formation of chips. The TFD is generally used to create a bushing on sheet metal, tubing, or/and thin-walled shapes for joining parts in an easy and effective way. In the present works, the AA6082 aluminium alloy sheets were drilled using TFD using different process variables, namely, the tool rotational speed (TRS), tool feed rate (TFR) and the tool conical angle (TCA). The influence of the abovementioned variables on the hole dimensional characteristics i.e., the hole diameter (HD), the bushing height (BH), and the bushing thickness (BT) were examined. The regression analysis and artificial neural network (ANN) approaches were applied to predict the hole dimensional characteristics. The results revealed that the developed ANN models were successfully used to predict the hole dimensional characteristics. While the linear regression models failed to the hole dimensional characteristics with an acceptable accuracy. The linear regression and ANN models for predicting the dimensional characteristics showed maximum mean average percentage error (MAPE) values of 46.30% and 16.46%, respectively.

1. Introduction

The thermal friction drilling (TFD) is a hole shaping process in metallic sheets [1,2]. The process uses the heat generated due to the friction between the workpiece and the rotating tool to produce the holes. During this process, there is no cutting fluid or lubricant is used. The TFD process has several applications in automotive industries such as in exhaust system parts, seat frame, fuel rail, seat handle, oxygen sensor and foot pedal [3,4].

Several TFD process parameters can affect the quality of the manufactured hole, namely, shape and geometry of drilling tool, workpiece and tool material properties, spindle speed, feed rate, and the thickness of workpiece [5]. The selection of proper values of these process parameters is very critical to produce enough heat needed to soften the workpiece materials and obtaining good quality holes. The quality of the drilled holes can be evaluated using several measurements like the hole diameter, height and thickness of bushing, surface roughness of the hole surface, and the formation of crack and damage in bushing.

There are few investigations were reported on the modelling and optimization of the TFD process variables [6-12]. In these investigations, several modelling and optimization techniques were used, typically, grey relation analysis (GRA), artificial neural networks (ANN), Taguchi design, fuzzy logic, …etc.]. For example, *Sushant* and *Vinayak* [7]

* Corresponding author. Tel: +201095613501.
E-mail address: mabdelhameed223@gmail.com

developed relationships using regression analysis between temperature developed in TFD and three input TFD process parameters, typically, temperature, thermal stress, and hardness as a function of material type, speed, and feed rate. *Pantawane* and *Ahuja* [9] studied the effect of TFD process parameters, namely, the rotational speed, feed rate and drilling tool diameter on the responses, namely, the dimensional error and surface roughness of the bush for AISI 1015 steel. The response surface methodology (RSM) was adopted to develop an empirical model for the responses as a function of TFD process parameters. *Kanagaraju et al.* [10] adopted the Taguchi approach to optimize and determine the influence of the TFD process variables of 6061-T6 aluminium alloys. Relationships between thrust force and TFD process variables was attained for the thrust force. *Rajesh et al.* [12] developed a predictive model for the predicting the bushing length using a feed-forward ANN based on experimental data. The optimization process was performed by implementing a genetic algorithm under constraint limits to maximize the bushing length. Moreover, a confirmation test was performed with the intention to compare the optimal value and its corresponding bushing length predicted by the genetic algorithm. Good agreement was noticed between the experimental and the predicted values.

In the present investigation, holes were drilled in 3 mm sheets made from AA6082 aluminum alloys using TFD process. The influence of the TFD process variables, typically, the TRS, TFR and TCA on the hole dimensional characteristics, including the HD, BH and BT were investigated. Regression and ANN models were developed to correlate the relationship between the TFD process variables and the hole dimensional characteristics. The developed ANN models are based on Multi-Layer Perceptron (MLP) and Radial Basis Function (RBF) neural networks approaches.

2. Experimental Procedures

2.1. Workpiece Material

Sheets made from AA6082 aluminum alloy (Al-Mg-Si-Cu) with 3 mm thickness were chosen as a workpiece material. Chemical composition of AA6082 aluminum alloy is listed in Table 1.

Table 1. Chemical composition of AA6082 aluminium alloy.

Alloy	Elements (wt. %)								
	Mn	Cu	Fe	Mg	Zn	Si	Cr	Ti	Al
AA6082	0.62	0.1	0.5	0.7	0.2	0.89	0.25	0.1	Bal.

2.2. Drilling Tool

In the current study, thermal friction drilling process was achieved using H13 tool steel having the chemical compositions listed in Table 2. TFD process was performed using three different drilling tools having three conical angles (β), namely, 30^o, 40^o and 50^o and a constant height of 15 mm. Figure 1 shows an illustration of the used drilling tools. Drilling tools have constant diameter of 15 mm at the cylindrical region.

Table 2. Chemical composition of H13 tool steel.

Alloy	Elements (wt.-%)						
	Cr	Si	Mo	V	Mn	C	Fe
H13	5.21	1.1	1.37	0.90	0.40	0.39	Bal.

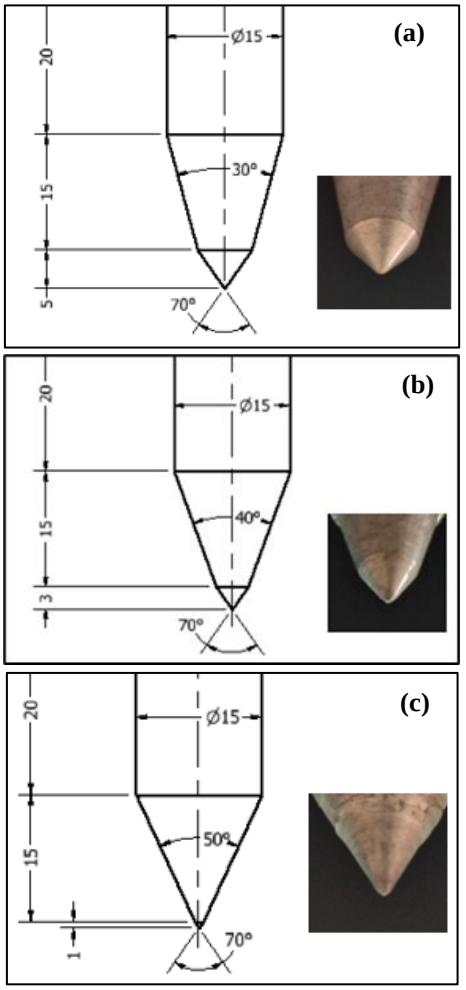

Figure 1. Drilling tools with different conical angles (β): (a) 30^o, (b) 40^o, and (c) 50^o.

2.3. Thermal Friction Drilling Process

TFD process was performed on AA6082 Al-sheets using different process variables i.e., TRS, TFR and TCA. Table 3 displays TFD process variables and their levels. After TFD, the workpieces were cross-sectioned at the center of the hole using wire-cut machine, later the hole dimensional characteristics i.e., HD and BH and BT were determined. Figure 2 shows a schematic illustration of the HD, BT and BH dimension hole characteristics. The dimensions of the holes were measured using *JMicroVision* image analyzing software. The measurements were conducted using a digital ruler. The accuracy of the linear measurements was 0.001 mm. Figure 3 shows a photograph of the TFD process and the experimental setup.

Table 3. Studied TD process parameters and their levels.

Parameter	Symbol	Unit	Level		
			Min.	Avg.	Max.
Feed Rate	TFR	mm/min.	100	200	300
Rotational Speed	TRS	rpm	2000	2500	3000
Conical Angle	TCA	Degree	30	40	50

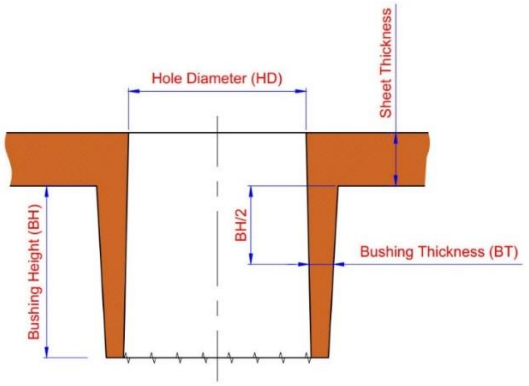

Figure 2. Bushing height, thickness, and hole diameter.

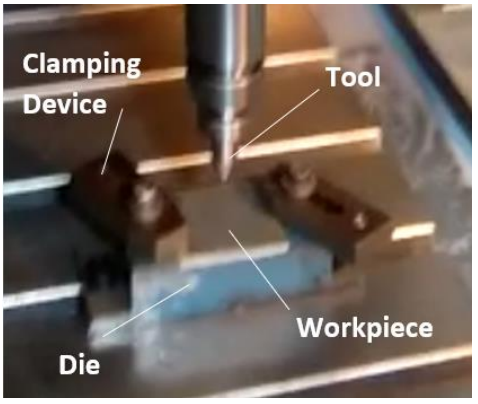

Figure 3. The experimental setup for TFD carried out in the present investigation.

The full factorial design of experiment (DoE) approach was adopted when performing the experiments. According to Table 3, the studied TFD parameters are three and each of these parameters has three levels (i.e., minimum, average and maximum). So, the total number of experiments to be conducted is 27 (3^3). Each experiment was replicated three times (i.e., the total number of observations is 27×3 =81) and the average value of the dimensional characteristics was determined. The analysis of variance (ANOVA) statistical approach was carried out to study the influence of the TFD process variables on the dimensional characteristics of the manufactured holes.

2.4. Regression Modelling

Regression analysis was utilized to correlate TFD process parameters i.e., TRS, TFR and TCA with hole characteristics dependent parameters i.e., HD, BH and BT. A linear regression function was developed, having the following general form:

$$y = b_o + b_1X_1 + b_2X_2 + ... + b_kX_k \quad (1)$$

where y is the predicted value of the dependent variable (y) for any given value of the independent variables (X_i), and b_i is the regression coefficients.

2.5. ANN Modelling

Multi-Layer Perceptron (MLP) and Radial Basis Function (RBF) ANN modelling techniques were implemented. ANN model consists of three layers of nodes as displayed in Fig. 4. These layers are the input, hidden, and output layers. The input layer has an input signal to be processed. The prediction task is made using the output layer. A random number of hidden layers which are located between the input and output layers are the actual computational engine of MLP and RBF.

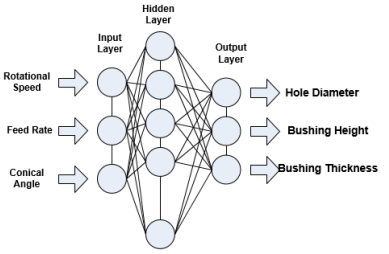

Figure 4. Schematic illustration of the general structure of ANN models.

The experimental data were divided into three sets, namely, training data set, test data set and validation data set. The training set represents (54 observations) was used to train the model. The validation set is smaller than the training set (14 observations). It is used to evaluate the performance of models as well as to detect overfitting during the training steps. The test set (13 observations) is used to get an idea of the final performance of a model.

The mean absolute percentage error (MAPE) was calculated to find the accuracy of the equations obtained from the regression and ANN models. The MAPE is given by the following formula -

$$MAPE = \frac{100\%}{n}\sum_{t=1}^{n}\left|\frac{A_t - F_t}{A_t}\right| \quad (2)$$

Where, A_t is the target (experimental) value and F_t is the predicted value. The difference between the above values is divided by A_t. The absolute value in this ratio is summed for every forecasted point in time and divided by the number of experimental data points *n*.

3. Results and Discussion

3.1. Shape of Holes and Bushing

Figure 5 displays typical examples of photographs of cross-sections of bushes formed after TFD of AA6082 Al-sheets using different TRS and TCA with constant TFR of 100 mm/min. Results revealed that TFD process variables play a substantial role in determining the final shape and dimension characteristics of the hole and bushing.

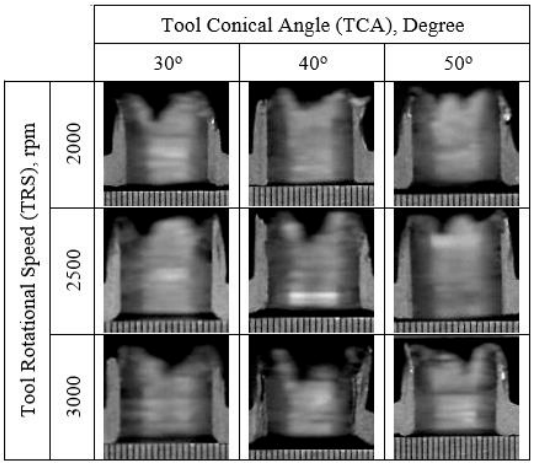

Figure 5. Typical examples of the photographs of the cross-sections of bushes formed after TFD at constant TFR of 100 mm/min and several TRS and TCA.

The smallest of HD was ≈ 14.992 mm for the holes drilled using TRS, TFR and TCA of, respectively, 2000 rpm, 200 mm/min and 60°. On the other hand, the largest HD was ≈ 15.296 mm for the holes drilled using TCA, TRS, and TFR of, respectively, 30°, 2000 rpm, 100 mm/min. The longest BH was ≈8.532 mm and was noted for the holes drilled using TCA, TFR and TRS of, respectively, 40°, 200 mm/min and 2000 rpm. The shortest BH was ≈ 6.875 mm and was noted for holes drilled using TRS, TCA, and TFR of, respectively, 2500 rpm, 40°, and 200 mm/min. According to these results, BH of the holes varies between 2.29 t and 2.844 t, where (t) is the sheet thickness. The thickest BT was ≈ 2.431 mm and observed for hole drilled using TCA, TRS and TFR of, respectively, 30°, 3000 rpm and 300 mm/min. The thinnest BT was ≈0.829 mm and was observed for hole drilled using TRS, TCA and TFR of, respectively, 2000 rpm, 50° and 200 mm/min.

3.2. The ANOVA Results

Figures 6-8 show main effect plots for HD, BH and BT, respectively. The results showed that, for the HD, increasing the TRS and/or TCA reduce(s) the diameter of the hole manufactured using TD process. Increasing the TFR from 100 to 200 mm/min reduced the HD, while increasing the TFR from 200 to 300 mm/min increased the HD, but still lower than the hole diameter resulted at TFR of 100 mm/min. Increasing the TRS and/or TCA reduce(s) the BH (see Fig. 7). While, increasing the TFR from 100 mm/min to 200 mm/min increased the BH, further increase in the TFR up to 300 mm/min tends to reduce the BH in the AA6082 Al alloy sheets. Moreover, increasing the TRS increases the BT, while increasing both the TFR and TCA reduce the BT (see Fig. 8). The increase in the TRS increases BT, but at the same time reduces the BH. This result is expected since the volume of the material is constant [1].

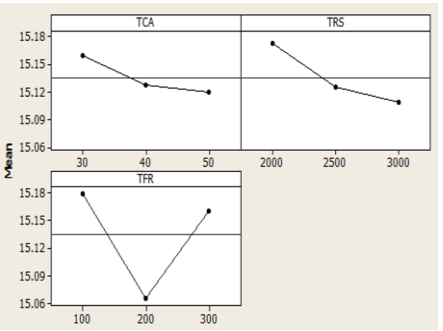

Figure 6. The main effect plots for HD in AA6082 Al alloy sheets manufactured using TFD.

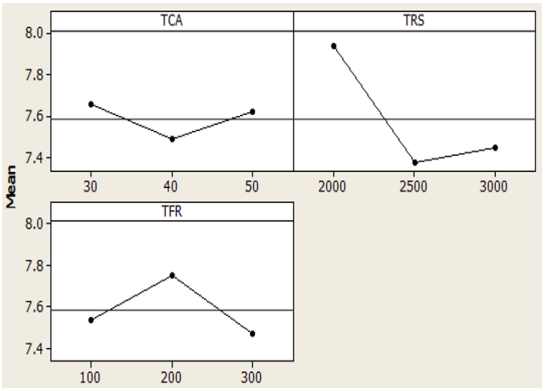

Figure 7. The main effect plots for BH in AA6082 Al alloy sheets manufactured using TFD.

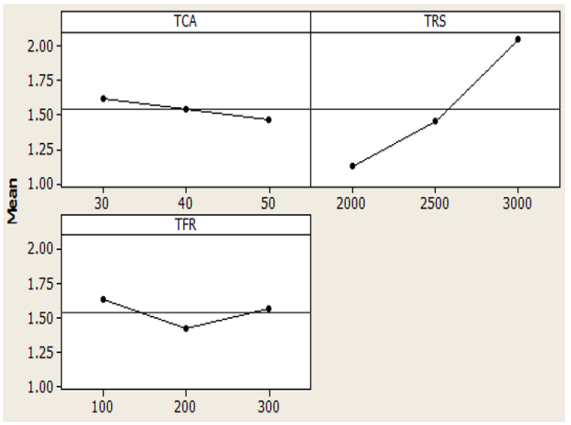

Figure 8. The main effect plots for BT in AA6082 Al alloy sheets manufactured using TFD.

3.3. Regression Model

Eqs. 3-5 show the results from linear regression modelling for HD, BH and BT, respectively.

$$HD = 15.4 - 0.00198\,TCA - 0.000064\,TRS - 0.000096\,TFR \quad (mm) \quad (3)$$

$$BH = 8.94 - 0.0018\,TCA - 0.000487\,TRS - 0.00034\,TFR \quad (mm) \quad (4)$$

$$BT = -0.399 - 0.00733\,TCA + 0.000919\,TRS - 0.000333\,TFR \quad (mm) \quad (5)$$

Where: HD, BH and BT are the hole diameter, bushing height, and bushing thickness, respectively in mm, The TCA is tool conical angle in degrees, TRS is the tool rotational speed in rpm, and TFR is the tool feed rate in mm/min. The results revealed that MAPE values of Eq. (3), Eq. (4) and Eq. (5) are 41.89%, 46.30% and 15.95%, respectively. These results indicate that the linear models are failed to model the dimensional characteristics of the holes with an acceptable accuracy, especially, for the HD and BH. Figures 9 show a comparison between the experimental and predicted HD, BH and BT resulted from linear regression models. The ideal prediction is obtained when the experimental and predicted points are coincident. For the HD and BH, the experimental and predicted points are not close to each other, while for the BT, these points are more relatively closer to each other. Ideal prediction is obtained when the experimental and predicted points are coincident. For HD and BH, the experimental and predicted points are not close to each other, but for BT, these points are more relatively closer to each other.

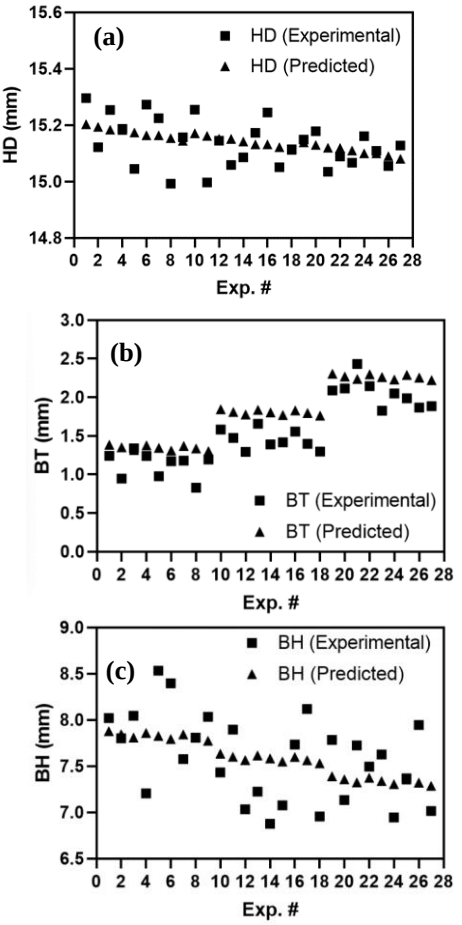

Figure 9. Comparison between the experimental and predicted (a) HD, (b) BH and (c) BT resulted from linear regression model.

3.4. ANN Model

Two models were developed based on MLP and RBF ANN techniques. The structure of the two neural networks consists of three layers, typically, input, hidden, and output layers. Both MLP and RBF networks have an input layer that consists of three nodes, namely, the TRS, TCA and TFR. Also, both

networks have an output layer that consists of three nodes, namely, the HD, BH and BT. The results revealed that best structure for the RBF and MLP networks have five and six nodes in the hidden layer, respectively. This indicates that the best performances were obtained for RBF and MLP models having structures 3-5-3 and 3-6-3, respectively. The activation functions used for the hidden layers of the MLP, and RBF networks were exponential and Gaussian functions, respectively. While the activation functions used for the output layers of the MLP, and RBF networks were Logistic and Identity (Linear) functions, respectively. The RBF network exhibited training, test, and validation performances of 63.031%, 72.905 and 56.970%, respectively. The MLP network exhibited training, test, and validation performances of 73.356%, 79.535 and 57.426%, respectively.

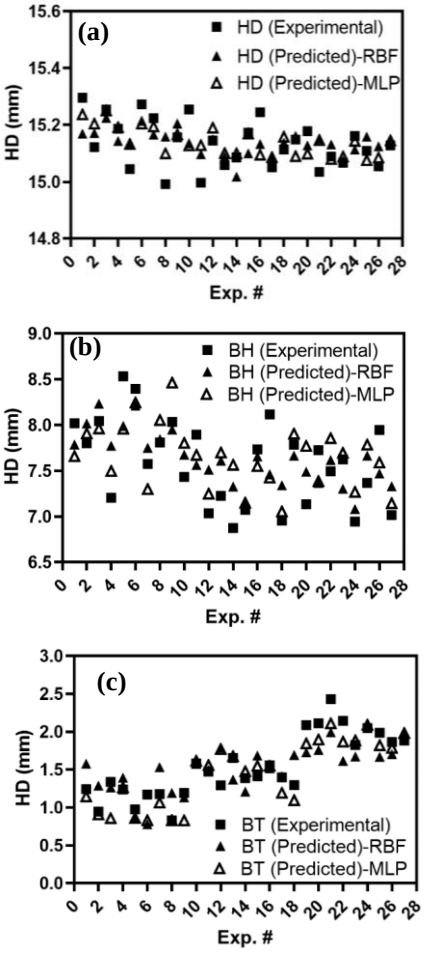

Figure 10. Graphical illustration for the relationship between experimental and predicted HD values resulted from RBF and MLP neural network models for (a) HD, (b) BH and (c) BT.

Figure 10 shows a graphical illustration for the relationship between the experimental and the predicted HD, BH and BT values resulted from the RBF and MLP neural network models. It has been found the MAPE resulted from the RBF and MLP neural network models for HD were 3.48% and 4.05%, respectively. The MAPE resulted from the RBF and MLP neural network models for BH were 3.84% and 4.06%, respectively. While the MAPE resulted from the RBF and MLP neural network models for BT were 16.46% and 10.88%, respectively. Based on the abovementioned results showed that good agreement was observed between the experimental and the predicted values.

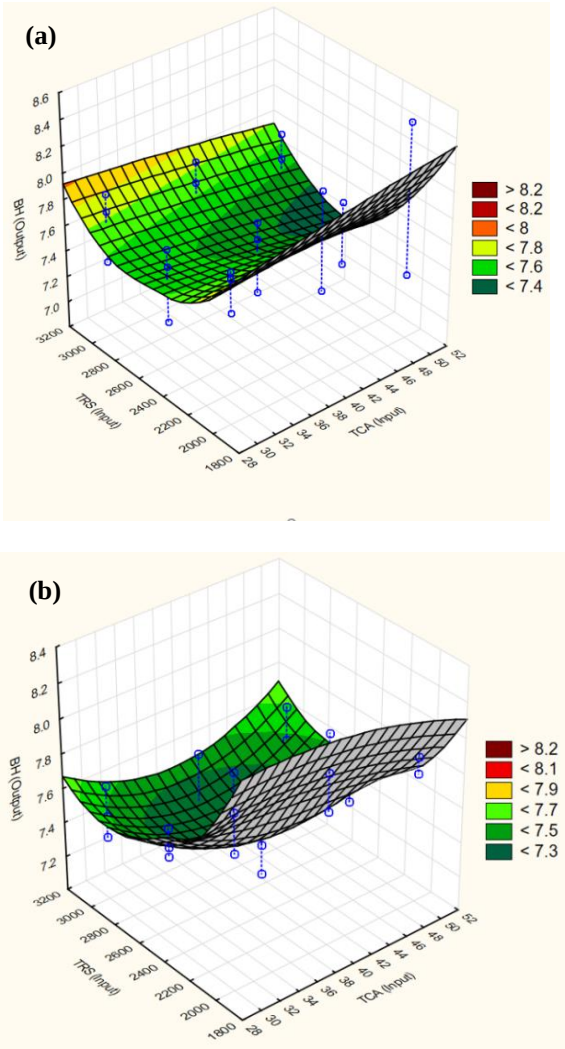

Figure 11. Three-dimensional surfaces show the variation of the BH with TRS, and TCA resulted from the (a) MLP and (b) RBF neural network models.

Figures 11 and 12 show typical three-dimensional surfaces that illustrate the variation of the BH with TRS, TFR and TCA resulted from the MLP as well as RBF neural network models. The MLP and RBF models showed that the dependence of the BH on both TFR, and TCA is very small (see Fig. 12). The 3D surfaces on these figures are very flat i.e., any change in the TFR and TCA did not have any significant influence on BH. The TRS exhibited the most significant influence on the dimensional characteristics of the holes. For example, the 3D surfaces show that, at constant TCA and TFR, any change in the TRS can influence the hole dimensional characteristics. The significance of the TRS on the dimensional characteristics as compared to the TFR and TCA was reported by many investigators [11-13].

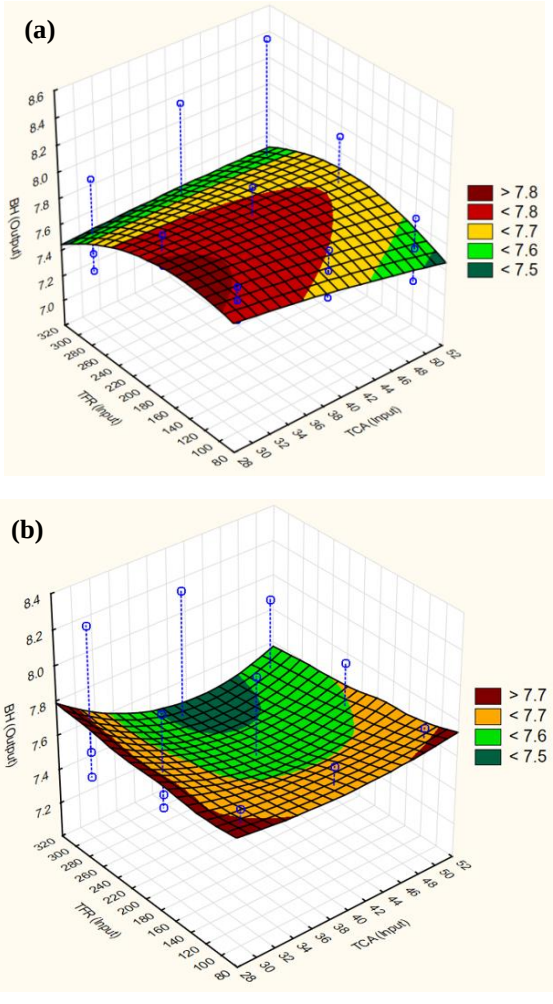

Figure 12. Three-dimensional surface shows the variation of the BH with TRS, and TCA resulted from the (a) MLP and (b) RBF neural network models.

4. Conclusions

Based on the obtained results, the following remarks can be drawn:

1. The developed linear regression models for predicting the hole dimensional characteristics, typically, HD, BH and BT showed MAPE values of 41.89%, 46.30% and 15.95%, respectively. The regression models were failed to predict the hole dimensional characteristics with acceptable accuracies due to the complex interaction between the thermal friction drilling process parameters.
2. Two ANN models based on the Multi-Layer Perceptron (MLP) and Radial Basis Function (RBF) approaches were developed. These ANN models were successfully used to predict the hole dimensional characteristics. For the HD, the MLP and RBF models exhibited mean average percentage error (MAPE) of about 3.48% and 4.05%, respectively. While for BH, the MAPE resulted from the RBF and MLP ANN models are 3.84% and 4.06%, respectively. The MAPE resulted from the RBF and MLP ANN models for prediction of the BT are 16.46% and 10.88%, respectively.
3. The ANN models showed good agreement between the predicted and the experimental values of the holes dimensional characteristics when compared with the linear regression models. The developed ANN models can be used to successfully predict the hole dimensional characteristics and reduce the tedious experimental work.

References

[1] Kumar R., Rajesh Jesudoss Hynes N., "Thermal Drilling Processing on Sheet Metals: A review", International Journal of Lightweight Materials and Manufacture, Vol. 2, pp. 193-205, 2019.

[2] Hamzawy N., Khedr M., Mahmoud T. S., EI- Mahallawi I., and Khalifa T., "Investigation of Temperature Variation During Friction Drilling of 6082 and 7075 Al-Alloys", Light Metals, The Minerals, Metals & Materials Series, A. Tomsett (ed.), pp. 471-477, 2020.

[3] Prabhu T., Arulmurugu A., "Experimental and Analysis of Friction Drilling on Aluminium and Copper", International Journal of Mechanical Engineering and Technology (1.1MET), Vol. 5, No. 5, pp. 123-132, 2014.

[4] Hamzawy N., Khedr M., Mahmoud T. S., EI-Mahallawi I., and Khalifa T. A., "Studying the Distribution of Hardness Values in Friction Drilled 7075 Al-alloy Sheets at Different

Conditions", IOP Conf. Series: Materials Science and Engineering, 1172, 012026, doi:10.1088/1757-899X/1172/1/012026K, 2021.

[5] Dehghan S., Ismail M. I. S., Ariffin M. K. A., Baharudin B. T. H. T., Sulaiman S., "Numerical Simulation on Friction Drilling of Aluminum Alloy", Mat.wiss. u. Werkstofftech., Vol. 48, pp. 241–248, 2017.

[6] Hanumantha Rao K., Gopichand A., Pavan Kumar N., Jitendra K., "Optimization of Machining Parameters in Friction Drilling Process", International Journal of Mechanical Engineering and Technology (IJMET), Vol. 8, No. 4, pp. 242–254, 2017.

[7] Patil S.S., Bembrekar V., "Optimization and Thermal Analysis of Friction Drilling on Aluminium and Mild Steel by using Tungsten Carbide Tool", International Research Journal of Engineering and Technology (IRJET), Vol. 3, No. 12, pp. 1468-1474, 2016.

[8] El-Bahloul S.A., El-Shourbagy H.E., El-Midany T.T., "Optimization of Thermal Friction Drilling Process Based on Taguchi Method and Fuzzy Logic Technique", International Journal of Science and Engineering Applications, Vol. 4, No. 2, pp. 55-59, 2015.

[9] Pantawane P.D., Ahuja B.B., "Experimental Investigations and Multi-Objective Optimization of Friction Drilling Process on AISI 1015" International Journal of Applied Engineering Research, Vol. 2, No. 2, pp. 448-461, 2011.

[10] Kanagaraju T., Peter J.S.J., Samuel D.R., and Prakash J. P., "Optimization of Drilling Parameters for Thrust Force and Torque in Friction Drilling Process", Middle East Journal of Scientific Research, Vol. 24, No. 4, pp. 1577-1582, 2016.

[11] Ku W.L., Hung C.L., Lee S.M., Chow H.M., "Optimization in Thermal Friction Drilling for SUS 304 Stainless Steel", Intternational Journal of Advanced Manufacturing Technology, Vol. 53, pp. 935-944, 2011.

[12] Hynes N.R.J., Kumar R., Sujana J.A.J., "Optimum Bushing Length in Thermal Drilling of Galvanized Steel using Artificial Neural Network Coupled with Genetic Algorithm", Materials and Technologies, Vol.51, No. 5, pp. 813-822, 2017.

[13] Ku W.L., Chow H.M., Lin Y.J., Wang D.A., Yang L.D., "Optimization of Thermal Friction Drilling Using Grey Relational Analysis", Advanced Materials Research, Vol. 154-155, pp. 1726-1738, 2011.